THE JOURNAL OF BIOLOGICAL CHEMISTRY VOL. 285, NO. 12, pp. 9211–9220, March 19, 2010

Crystal Structure of the Mp1p Ligand Binding Domain 2 Reveals Its Function as a Fatty Acid-binding Protein*

Received for publication, August 19, 2009, and in revised form, December 7, 2009 Published, JBC Papers in Press, January 6, 2010, DOI 10.1074/jbc.M109.057760

Shuang Liao[‡§], Edward T. K. Tung[¶], Wei Zheng[‡], Ken Chong[§], Yuanyuan Xu[‡], Peng Dai[‡], Yingying Guo[‡], Mark Bartlam[‖], Kwok-Yung Yuen[¶1], and Zihe Rao[‡§‖2]

From the [‡]Laboratory of Structural Biology, Tsinghua University, Beijing 100084, China, the [¶]State Key Laboratory of Emerging Infectious Diseases, The University of Hong Kong, Hong Kong, the [§]National Laboratory of Macromolecules, Institute of Biophysics, Chinese Academy of Science, Beijing 100101, China, and the [‖]Tianjin Key Laboratory of Protein Science, College of Life Sciences, Nankai University, Tianjin 300071, China

Penicillium marneffei **is a dimorphic, pathogenic fungus in Southeast Asia that mostly afflicts immunocompromised individuals. As the only dimorphic member of the genus, it goes through a phase transition from a mold to yeast form, which is believed to be a requisite for its pathogenicity. Mp1p, a cell wall antigenic mannoprotein existing widely in yeast, hyphae, and conidia of the fungus, plays a vital role in host immune response during infection. To understand the function of Mp1p, we have determined the x-ray crystal structure of its ligand binding domain 2 (LBD2) to 1.3 Å. The structure reveals a dimer between the two molecules. The dimer interface forms a ligand binding cavity, in which electron density was observed for a palmitic acid molecule interacting with LBD2 indirectly through hydrogen bonding networks via two structural water molecules. Isothermal titration calorimetry experiments measured the ligand binding affinity (K_d) of Mp1p at the micromolar level. Mutations of ligand-binding residues, namely S313A and S332A, resulted in a 9-fold suppression of ligand binding affinity. Analytical ultracentrifugation assays demonstrated that both LBD2 and Mp1p are mostly monomeric *in vitro*, no matter with or without ligand, and our dimeric crystal structure of LBD2 might be the result of crystal packing. Based on the conformation of the ligand-binding pocket in the dimer structure, a model for the closed, monomeric form of LBD2 is proposed. Further structural analysis indicated the biological importance of fatty acid binding of Mp1p for the survival and pathogenicity of the conditional pathogen.**

Penicillium marneffei is an important pathogenic fungus found in Southeast Asia. In most cases, it afflicts only immunocompromised individuals, such as AIDS patients, causing respiratory, skin, and systemic mycosis. As a conditional pathogen, *P. marneffei* is unique for its thermal dimorphic feature. It undergoes a phase transition, from the mold phase (filamentously) at room temperature (25 °C) to the uninucleate yeast form at body temperature (37 °C). Infecting nearly 10% of AIDS patients in southeast Asia, where it is most entrenched, penicilliosis infection has gradually been recognized as the third most common indicator of AIDS following tuberculosis and cryptococcosis in northern Thailand (1). Given the global prevalence of AIDS, *P. marneffei* may provide an optimal model for research into the molecular mechanisms of pathogenic fungi relating to pathogenesis, virulence, and interactions with the host immune system.

Despite its medical importance and interesting characteristics as a dimorphic fungus, knowledge of the molecular mechanisms underlying the pathogenesis of *P. marneffei* remains limited, in part because of the lack of a completely annotated and sequenced genome. Nonetheless, Mp1p is the first characterized cell wall mannoprotein of *P. marneffei* and has been successfully used in serodiagnosis and prevention of the resulting infection (2–6). It is an antigenic cell wall mannoprotein present in the cell wall of yeast, hyphae, and conidia of *P. marneffei*. Residues 22–180 of Mp1p share high similarity (53% identities and 74% positives) with residues 187–346. Consequently, Mp1p can be divided into three independent domains. Ligand binding domains 1 (LBD1, residues 22–180)[3] and 2 (LBD2, residues 187–346) bear superficial structural similarity based on sequence alignment, whereas the last domain is serine- and threonine-rich and may be highly glycosylated *in vivo*. There is a signal peptide at the N terminus and a putative glycosylphosphatidylinositol attachment signal sequence at the C terminus of Mp1p. High levels of antibodies produced specifically against Mp1p are detected in the sera of penicilliosis patients, indicating an important role of Mp1p in the host humoral immune process (3). Mp1p is also detected in the culture supernatants of *P. marneffei* and in the sera of penicilliosis patients. Both *in vitro* and *in vivo* findings suggest that Mp1p is an abundantly secreted protein. Therefore, a combination of antigen and antibody tests was used for better diagnosis of penicilliosis. Beyond its role in diagnostic testing for this disease, *MP1*-based DNA vaccine was demonstrated to produce a pro-

* This work was supported by Ministry of Science and Technology 973 Project Grants 2006CB10901 and 2007CB914301) and 863 Project Grant 2006AA02A322, and International Cooperation Project Grant 2006DFB32420.

[1] To whom correspondence may be addressed: State Key Laboratory of Emerging Infectious Diseases, The University of Hong Kong, Hong Kong. Tel.: 852-28554892; Fax: 852-28551241; E-mail: kyyuen@hkucc.hku.hk.

[2] To whom correspondence may be addressed: Laboratory of Structural Biology, New Life Sciences Bldg., Tsinghua University, Beijing 100084, China. Tel.: 86-10-62771493; Fax: 86-10-62773145; E-mail: raozh@xtal.tsinghua.edu.cn.

[3] The abbreviations used are: LBD, ligand binding domain; GC/MS, gas chromatography/mass spectrometry; ITC, isothermal titration calorimetry; AUC, analytical ultracentrifugation; WT, wild type; MES, 4-morpholineethanesulfonic acid; MALDI-TOF, matrix-assisted laser desorption ionization time-of-flight; PA, palmitoleic acid; Wat, water molecule.

tective immune response against *P. marneffei* challenge in a mouse model (7).

To improve our understanding of the function of Mp1p in *P. marneffei*, we determined the three-dimensional structure of its LBD2 by x-ray crystallography. Taking advantage of high quality data, a ligand was identified to bind Mp1p and could be interpreted from the electron density as a fatty acid molecule, which was determined to be a mixture of fatty acids (mostly palmitic acid and stearic acid) by gas chromatography/mass spectrometry (GC/MS). As the natural host of *P. marneffei*, macrophages are able to deprive intracellular pathogens of required nutrients for microbial killing (7). Not surprisingly, intracellular pathogens residing within macrophages have developed a similar mechanism to cope with nutrient deprivation: induction of the glyoxylate cycle, a pathway that permits the utilization of compounds with two carbons (C2 compounds), to satisfy cellular carbon requirements (8). This is also true for *P. marneffei*, and the pathway allows the utilization of fatty acids as a carbon source for *P. marneffei* in macrophages. The *AcuD* gene, which encodes an important enzyme within the glyoxylate cycle, is regulated by both carbon source and temperature in *P. marneffei* (9). In addition to serving as a carbon source for the pathogens, lipids are also involved in many other processes, such as signaling during exocytosis, inflammation, and immune response (10, 11). Isothermal titration calorimetry (ITC) experiments further confirmed the fatty acid binding capability of Mp1p, implying that Mp1p may serve as a fatty acid transporter between the pathogen and host cells during infection.

EXPERIMENTAL PROCEDURES

Cloning and Expression—The DNA coding sequence of wild type Mp1p residues 35–429 (with the N-terminal signal peptide and C-terminal glycosylphosphatidylinositol sequence truncated) and LBD2 (residues 187–346) were cloned into the pET-28a vector (Novagen) between the BamHI and XhoI sites. Point mutations of full-length Mp1p (P254A and P255A) and LBD2 (I207M, L276M, S313A, and S332A) were produced from the constructed pET-28a-Mp1p-187–346 plasmid with a one-step overlap extension PCR method using the Easy mutagenesis system kit (Transgen).

All of the Mp1p variants were expressed as N-terminal His_6-tagged proteins in *Escherichia coli* BL21(DE3) in LB medium. A selenomethionyl derivative was expressed in a $metE^-$ *E. coli* host strain B834 (Novagen) in M9 minimal medium supplemented with 30 mg of selenomethionine/liter.

For expression, *E. coli* cells cultured overnight were diluted 100-fold in fresh medium and cultured at 37 °C to an optical density of ~0.8 at 600 nm. The cell culture was then cooled to 16 °C and induced with 0.5 mM isopropyl β-D-1-thiogalactopyranoside. It was then grown for another 20 h at 16 °C with shaking at 220 rpm before cells were harvested by centrifugation.

Protein Purification—Harvested cells were resuspended in buffer A (20 mM MES, pH 5.5, 500 mM NaCl, 10% (v/v) glycerol) and lysed by sonication. The released His_6-tagged protein was purified following standard protocols of nickel-nitrilotriacetic acid resin (Qiagen). His_6-tagged protein was eluted from the resin with buffer B (20 mM MES, pH 5.5, 500 mM NaCl, 10% (v/v) glycerol, and 100 mM imidazole) and dialyzed against a salt-free buffer (20 mM MES, pH 5.5). Further purification was performed with a Resource S column (GE Healthcare) and then a Superdex 75 column (GE Healthcare). The resulting fraction was dialyzed against a buffer containing 20 mM MES, pH 5.5, and 100 mM NaCl.

Crystallization—Crystallization carried out with full-length protein yielded crystals at 16 °C after a period of 1–2 months. SDS-PAGE of crystals revealed a dominant band at 16 kDa, indicating the possibility of degradation during crystallization. The 16-kDa band was subjected to N-terminal sequencing, and MALDI-TOF mass spectrometry analysis was carried out using the protein sample after incubation at 4 °C for 30 days. The results from N-terminal sequencing and MALDI-TOF mass spectrometry confirmed that the crystallized protein was LBD2 (residues 187–346) of Mp1p. Residues 170–319 of Mp1p share 99% identity with the full-length MP1 protein (*P. marneffei*, GenBank™ accession number AAZ80301.1), suggesting that this region is an independent functional domain. The protein fragment formed in our crystals contains most of the residues in this region (residues 187–319), with the exception of 17 residues at the N terminus (residues 170–186). A truncated construct of the LBD2 of Mp1p (residues 187–346) was thus designed for crystallization. Additionally, I207M and L276M mutations were incorporated into the construct for an increased selenium anomalous signal. Protein fractions were concentrated to 40 mg/ml in 20 mM MES, pH 5.5, 100 mM NaCl for further crystallization trials. The crystals of the native and selenomethionyl-labeled protein were grown by the hanging drop vapor diffusion method. The reservoir contained 11% polyethylene glycol 8000, 0.1 M HEPES, pH 7.5, 8% ethylene glycerol. A typical hanging drop consisted of 1 μl of protein solution (40 mg/ml) mixed with 1 μl of the reservoir solution. Large colorless diamond-shaped crystals with optimal diffraction quality were obtained within 3 days at 16 °C.

Data Collection, Phasing, and Model Refinement—Diffraction data from a native protein crystal were collected in-house with a Rigaku MM-007 x-ray generator and a Rigaku R-AXIS IV++ detector at 100 K. Data for the selenomethionyl-derivative protein crystal were collected on Beamline BL5A of the Photon Factory synchrotron facility (KEK, Tsukuba, Japan). The raw data were indexed, integrated, and scaled using the HKL2000 program suite (12). A 1.3-Å resolution structure of the selenomethionyl-labeled Mp1p was solved by the single-wavelength anomalous diffraction phasing method at the selenium absorption edge using SOLVE/RESOLVE (13). The majority of the structure was built automatically by the program ARP/WARP (14). The remainder of the structure was completed by further manual building and refinement with COOT (15) and Refmac5 (16), respectively. The figures were prepared with the program PYMOL (DeLano Scientific, San Carlos, CA).

Delipidation and Calorimetric Binding Assays—Purified full-length Mp1p protein, the LBD2, and its S313A/S332A mutant forms were delipidated by extracting 500 μl of protein solution three times with 200 μl of diisopropylether:*n*-butanol (3:2) for 30 min with gentle shaking. The protein was then dialyzed against a calorimetry buffer (20 mM Tris, pH 8.0) to remove

n-butanol (17). Lipid binding assays were carried out using a Nano ITC^{2G} isothermal titration calorimeter (TA Instruments) at the Institute of Microbiology of the Chinese Academy of Sciences (Beijing, China). After delipidation and dialysis, the protein in the calorimetry buffer was adjusted to 100 μM for all reactions and titrated with the ligands up to 1.5-fold molar excess. The ligand was weighed into a 1.5-ml microreaction tube and dissolved in 250 mM NaOH to give a concentration of 100 mM and further diluted with calorimetry buffer into 1.5 mM stock solution for the operation. In a typical experiment the ligand stock solution was injected in 25 aliquots (10 μl each) in 5-min intervals at 25 °C. Raw data were processed by the NanoAnalyze software package supplied by the manufacturer. After the heat of dilution was subtracted from the heat of binding, the data were fitted to a model assuming one (for second domain) or two independent (for full-length) binding sites, and the values for enthalpy and binding affinity were subsequently obtained.

Analytical Ultracentrifugation (AUC)—AUC assays were performed with the sedimentation velocity method using a ProteomeLab XL-I protein characterization system (Beckman Coulter) operating at 55,000 rpm for Mp1p and 60,000 rpm for LBD2 at 20 °C at the Institute of Biophysics of the Chinese Academy of Sciences (Beijing, China). The Mp1p samples for AUC were prepared at a concentration of 4 mg/ml in a buffer containing 20 mM Tris-HCl, pH 8.0, 150 mM NaCl, and LBD2 at 4 mg/ml in 20 mM MES, pH 5.5, 150 mM NaCl. The protein samples were purified and delipidated as mentioned above. The AUC data were processed according to a c(M) distribution model (18).

GC/MS—The lipids were extracted from an aliquot of LBD2 with chloroform/methanol (2:1 v/v). The extract was then treated with an aliquot of methanolic HCl for 1 h at room temperature to produce the methyl ester of the hypothesized fatty acids. After the reaction, the derivatized sample was then analyzed by GC/MS on a Thermo Fisher DSQ instrument in the Analysis Center at Tsinghua University. The analyses were eluted from a 30m-long AB-5MS column by increasing the column temperature from 100–300 °C at 5 °C/min. The mass spectra were acquired using a scan range of 35–650 Da at 1000 scans/s.

RESULTS

Structure Determination and Refinement Reveals the Bound Ligand—The structure of the engineered LBD2 of Mp1p (I207M/L276M) was solved to 1.3-Å resolution using the single-wavelength anomalous diffraction method as described. The crystal belongs to the space group $P4_12_12$ with one molecule/asymmetric unit. Refinement of the LBD2 structure resulted in a final model with a crystallographic *R*-factor (R_{cryst}) of 0.182 and a free *R*-factor (R_{free}) of 0.197 (Table 1). The final model contains 153 amino acid residues (residues 194–346 in the native protein). The polypeptide chain was complete with the exception of the N-terminal His_6 tag and the N-terminal residues 187–193, which were not included in the final model because of poor electron density. In the crystal, LBD2 exists as a dimer with approximate dimensions of 25 × 40 × 80 Å^3, with two fatty acid ligands, which were revealed to be a mixture of fatty acids by GC/MS analysis (Fig. 1), inserted between the two molecules. To determine the identity of the LBD2 ligand, a purified preparation of LBD2 was extracted with chloroform/methanol (2:1) to isolate any bound organic compounds. The extract was then treated with methanolic HCl to convert the carboxylic acids groups to their corresponding methyl esters. The molecular weights for the constituents in the LBD2 extract, determined from the GC/MS data, were consistent with their identification as methyl esters of saturated and monounsaturated C16 and C18 fatty acids, mostly palmitic acid (C16:0) and stearic acid (C18:0) and some oleic acid (18:1) as well, although some 11-methoxyoctadocanoate, an uncommon fatty acid in *E. coli*, was also observed. The lack of electron density for the C10–12 atoms in the original density map is likely due to the mixture of fatty acids present in the crystal. Because it constitutes the majority of the fatty acids mixture (approximately two of three), palmitic acid was thus modeled into our final structure as a ligand.

TABLE 1
Data collection and refinement statistics

Parameter	Selenomethionyl LBD2
Data collection	
Space group	$P4_12_12$
Cell dimensions *a*/*b*/*c* (Å)	46.51/46.51/149.38
Wavelength (Å)	0.97894
Resolution (Å)	19-1.3 (1.35-1.3)
Average $I/\sigma(I)$	62.3 (5.5)
Total reflections	837,700
Unique reflection	41,553
Completeness (%)	99.9 (99.9)
Redundancy	20.2 (16.2)
R_{merge} [a]	0.079 (0.383)
Structure refinement	
R_{work} [b]	0.182
R_{free} [b]	0.197
Root mean square deviation from ideal geometry	
Bonds (Å)	0.007
Angles (°)	1.043
Average B factor (Å^2)	
Protein	11.258
Solvent	24.961
Ligand	25.486
Ramachandran plot (%) [c]	99.3/0/0

[a] $R_{merge} = \Sigma_h\Sigma_i|I_i(h) - \langle I(h)\rangle|/\Sigma_h\Sigma_i I_i(h)$, where $\langle I\rangle(h)$ is the mean of the observations $I_i(h)$ of reflection *h*.
[b] $R_{work} = \Sigma_h(||F_{obs}| - |F_{calc}||)/\Sigma I_h|F_{obs}|$; R_{free} is the *R*-factor for a subset (10%) of reflections that was selected before refinement calculations and not included in the refinement.
[c] Ramachandran plots were generated using SFCHECK.

Monomer Structure—The crystal structure reveals that the LBD2 is predominantly α-helical (Fig. 2*A*). One anti-parallel helical bundle comprised of two long helices is located at the N terminus and another anti-parallel helical bundle comprised of four helices is located at the C terminus. The two helical bundles are linked by a long loop and a small helix, which perhaps acts as a hinge to provide high flexibility during the ligand binding process. The whole molecule forms a flattened structure with two helical bundles in opposite orientations. The surface charge distribution of the monomer shows a high percentage of hydrophobic surface area, which is further explained in the dimer as a potential ligand binding interface. The overall structure exhibits no homology with existing structures in the Protein Data Bank (19) according to the DALI server (20), indicating a novel fold for fatty acid-binding protein. Based on the sequence similarity between LBD1 and LBD2 of Mp1p, a struc-

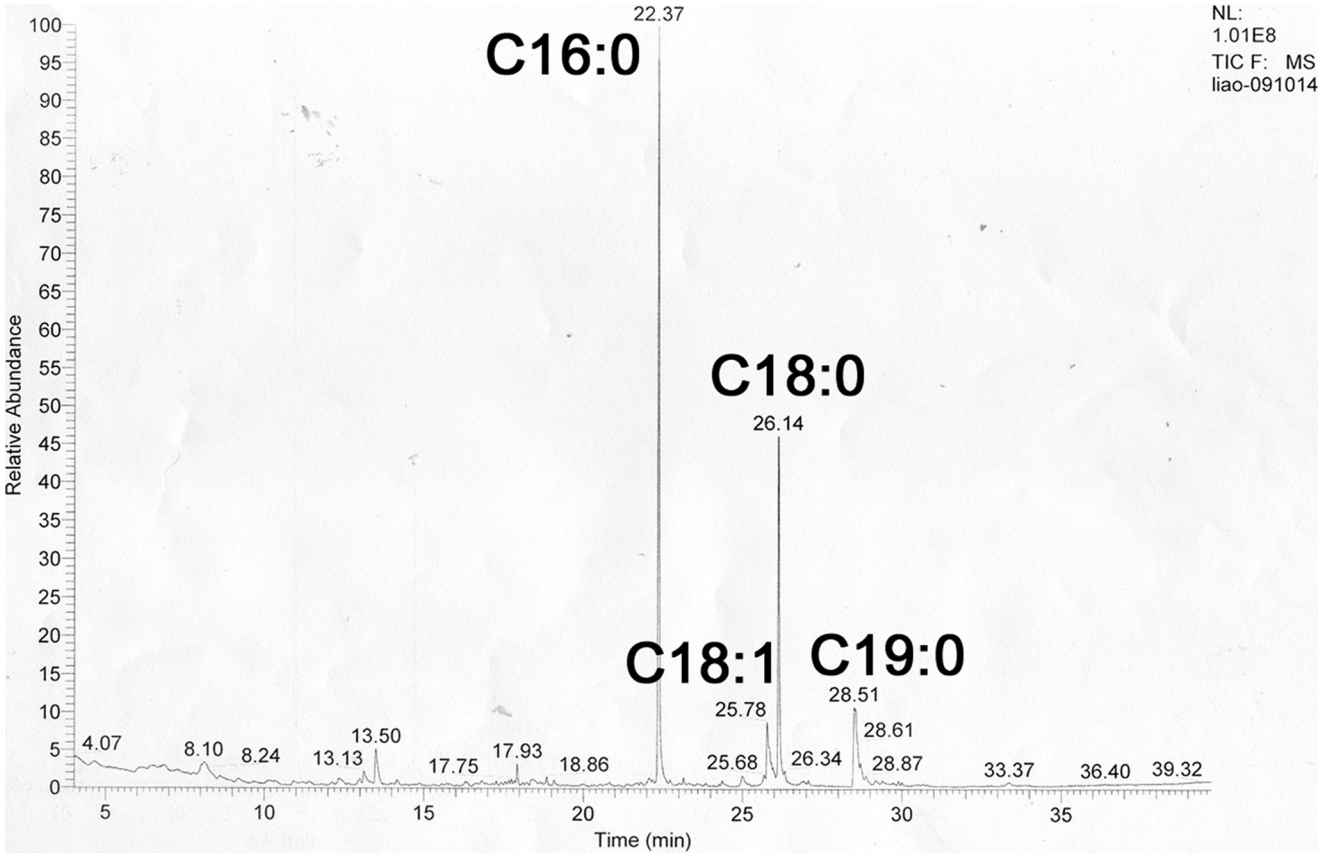

FIGURE 1. **GC/MS determination of LBD2 ligands.** Fatty acid chain lengths and saturation states are indicated.

tural model was constructed based on our crystal structure of LBD2 (Fig. 2*D*).

Dimer Structure—To elucidate the oligomerization state of LBD2 and MP1P, AUC experiments were carried out with both proteins. Because of the insoluble nature of palmitic acid, palmitoleic acid was thus used as a test ligand in the AUC experiments. AUC experiments suggest that the expressed Mp1p protein existed mainly as a monomer in solution, and less than 10% of the protein forms a 90-kDa homodimer (Fig. 3*A*). Although Mp1p was still mostly monomeric after delipidation (Fig. 3*B*) or addition of palmitoleic acid at a molar ratio of 1:2 (Fig. 3*C*), raising the molar ratio to 1:8 caused an obvious promotion of dimer formation (Fig. 3*D*). It is almost the same as LBD2, which was also monomeric with ligand at a 1:1 molar ratio (Fig. 3*G*) or without ligand (Fig. 3*F*) and only polymerized when there was excessive ligand in the protein solutions (Fig. 3*H*). It would seem that dimerization of Mp1p is not a requirement for ligand binding and thus may not be biologically relevant. Because there is a limited source of fatty acids in the natural host of *P. marneffei*, Mp1p may exist only as monomers *in vivo*.

In the crystal structure, two symmetry-related LBD2 molecules (termed subunits A and B) form an intertwined dimer with two rugby ball-like structures (Fig. 2*B*). Each of the rugby balls contains one ligand-binding pocket within the helical bundles, including helices from both subunits A and B. The ligand binding cavity of LBD2 consists mainly of hydrophobic residues, suggesting that the two subunits in the given dimer associate with the palmitic acid ligand largely via hydrophobic interactions. In addition to these hydrophobic interactions, a series of hydrogen bonds between residues from two subunits also help to stabilize the dimer. These include hydrogen bonds between the following pairs of residues: $Glu^{137A/B}$ and $Ser^{72B/A}$; $Asn^{115A/B}$ and $Asn^{51B/A}$; $Gln^{11A/B}$ and $Ser^{25B/A}$; $Asn^{95A/B}$ and $Glu^{36B/A}$; and $Thr^{8A/B}$ and $Glu^{36B/A}$. Structural water molecules (namely Wat^{9}, Wat^{16}, Wat^{20}, Wat^{32}, Wat^{41}, Wat^{81}, Wat^{122}, Wat^{126}, and Wat^{203}) also help to form a hydrogen bonding network between the two LBD2 molecules during dimerization. One of them, namely Wat^{32}, resides within the ligand binding cavity (Fig. 4*B*). Approximately 1,020 $Å^2$ (30%) of the solvent-accessible surface area from each subunit is buried upon dimer formation. Most of this buried area is composed of hydrophobic residues, many of which make direct contact with the hydrophobic backbone of the ligand.

Ligand Binding Cavity—An *R*-factor below 0.25 was obtained directly after model building by ARP/WARP against the 1.3 Å data. Upon careful refinement, a snake-like segment of electron density was found with a clear head group that could be fitted by a carboxylate group. Based on the high quality of the crystallographic data and the observation that palmitic acid is present in the *E. coli* host as an essential lipid, we comfortably fit the coordinates of palmitic acid into the corresponding density in the original single-wavelength anomalous diffraction phased map generated by RESOLVE (Fig. 4*B*). In the final model, the *B*-factor of the ligand is 25.5 $Å^2$, whereas the overall *B*-factor of the protein is 11.3 $Å^2$ (refined with Refmac5 with the occupancy of all atoms set to 1.0), which further shows the

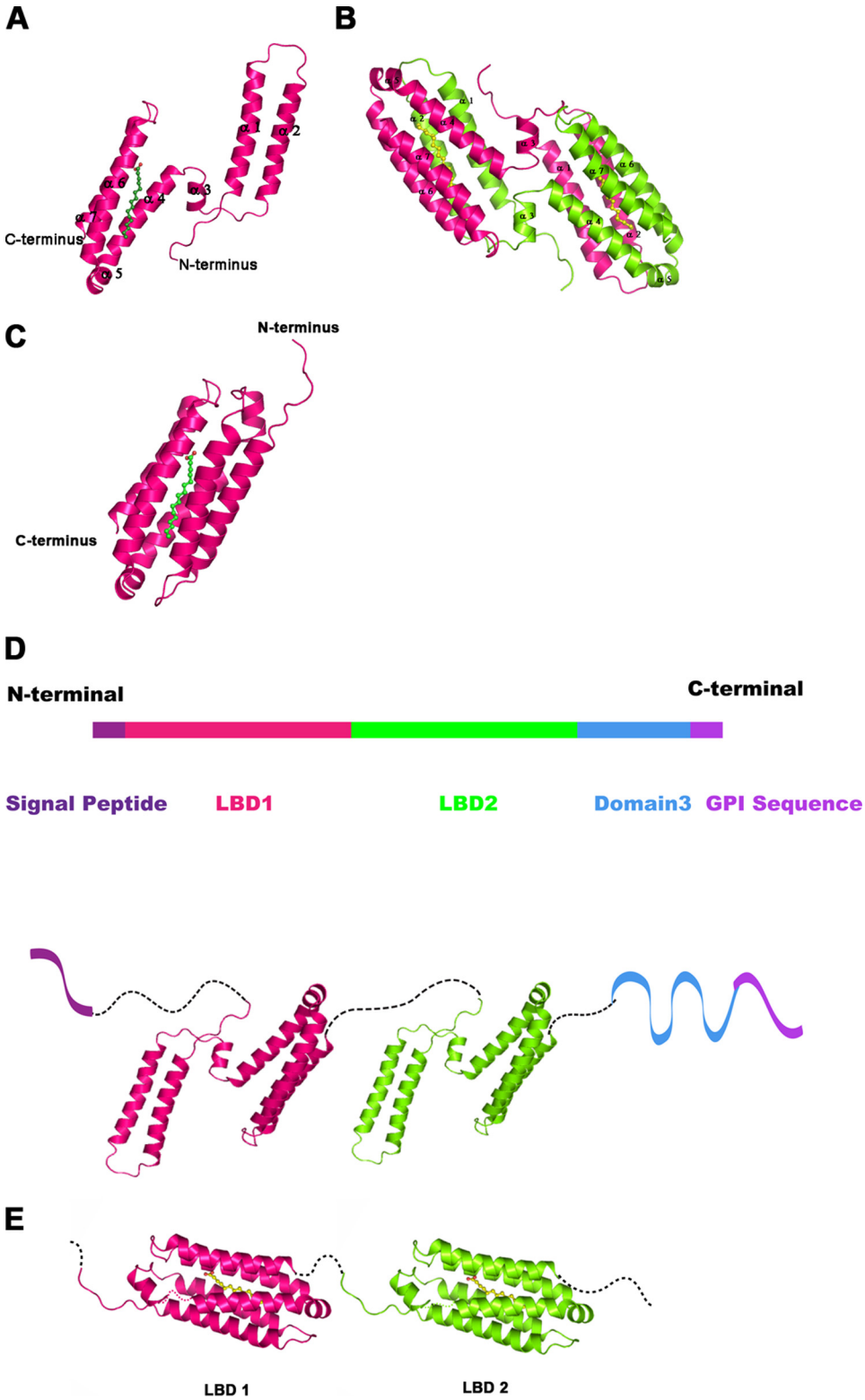

FIGURE 2. **Overall structure of the Mp1p LBD2, structural model for full-length Mp1p, and the possible conformation changes during ligand binding.** *A*, a ribbon diagram of the LBD2 monomer. The ribbon diagram is shown with the protein molecule colored *pink* and the palmitic acid ligand colored *green*. *B*, a ribbon diagram of the LBD2 homodimer. The two protein molecules are colored *pink* and *chartreuse*, respectively, and palmitic acid is colored *yellow*. *C*, a schematic for the closed form of the ligand-bound LBD2 monomer. The LBD2 molecule is colored *pink* and shown in ribbon representation; palmitic acid is colored *green*. The crystal structure of the LBD2 dimer is used as a model for the closed form conformation. *D*, a structural model for full-length Mp1p. The N-terminal signal peptide and C-terminal glycosylphosphatidylinositol sequence are colored *purple*. LBD1 and LBD2 are colored *pink* and *green*, respectively, and are shown in cartoon using the crystal structure of LBD2. The third domain is colored *blue*. The model is a schematic of Mp1p structure, not an interpretation of the real domain interactions in full-length protein. *E*, a schematic diagram for the possible conformation of Mp1p LBD1 and LBD2 domains bound with palmitic acid. The two LBD domains are colored *pink* and *green*, respectively, and palmitic acid molecules are colored *yellow*.

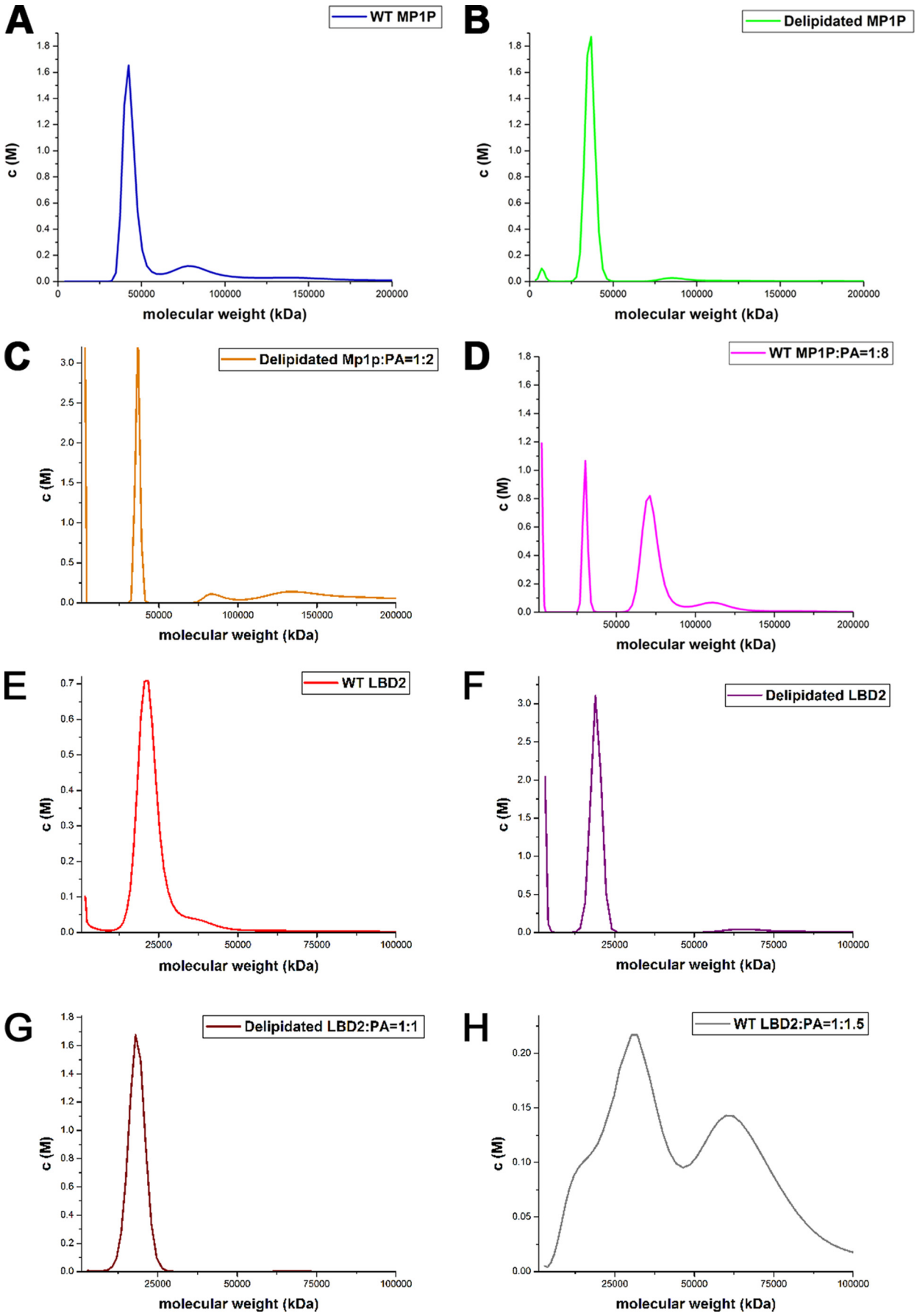
A
WT MP1P
c (M)
molecular weight (kDa)
B
Delipidated MP1P
c (M)
molecular weight (kDa)
C
Delipidated Mp1p:PA=1:2
c (M)
molecular weight (kDa)
D
WT MP1P:PA=1:8
c (M)
molecular weight (kDa)
E
WT LBD2
c (M)
molecular weight (kDa)
F
Delipidated LBD2
c (M)
molecular weight (kDa)
G
Delipidated LBD2:PA=1:1
c (M)
molecular weight (kDa)
H
WT LBD2:PA=1:1.5
c (M)
molecular weight (kDa)

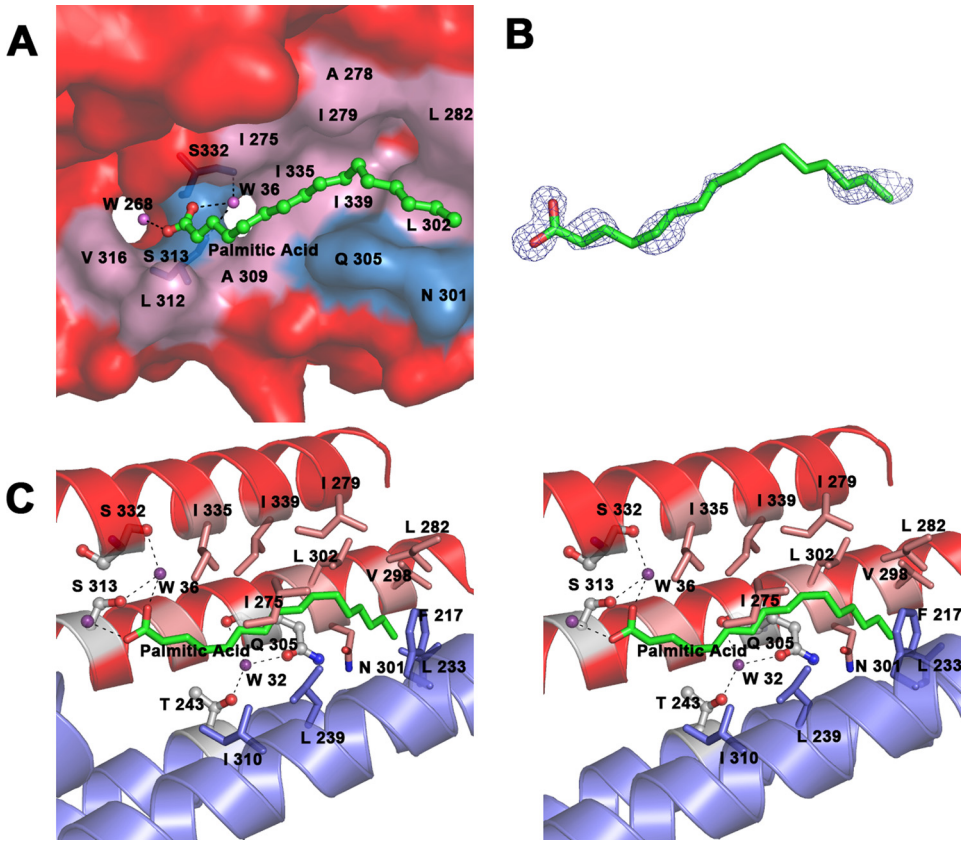

FIGURE 4. *A*, surface representation of Mp1p LBD2 in complex with palmitic acid. Palmitic acid is shown in ball-and-stick representation and colored by atom type (carbon in *green* and oxygen in *red*.) Water molecules are shown as *purple spheres*. Residues at the ligand binding site are labeled; the surface is colored *pink* for hydrophobic residues and *blue* for the rest. Surface residues outside the ligand binding site are colored *red*. Residues involved in hydrogen bonding networks are shown in stick representation. The *dashed lines* show the hydrogen bonds between the residues and water molecules. *B*, palmitic acid overlaid by a $2F_o - F_c$ electron density map contoured at 1.0 σ. Palmitic acid is shown in stick representation and colored by atom type (carbon in *green* and oxygen in *red*). The density map comes from the original single-wavelength anomalous diffraction phased map generated by RESOLVE. *C*, stereo view of the ligand binding site of Mp1p LBD2. Palmitic acid is colored by atom type (carbon in *green* and oxygen in *red*). Water molecules are shown as *purple spheres*. Residues involved in hydrogen bonding networks are shown in ball-and-stick representation and colored by atom type (carbon in *white*, oxygen in *red*, and nitrogen in *blue*). Residues forming hydrophobic interactions with palmitic acid are colored by atom types (carbon in *pink* and *blue* for subunits A and B, respectively; oxygen in *red*; and nitrogen in *blue*). The helixes are shown as a ribbon diagram and colored *red* and *blue* for subunits A and B, respectively. The *dashed lines* show the hydrogen bonds between the residues and water molecules.

reliability of our ligand model. In a given LBD2 dimer, the ligand lies in the valley of helical bundle a (the four-helix bundle) from subunit A, whereas helical bundle b (the two-helix bundle) from subunit B covers this interface from the opposite site to form a complete binding cavity. The two helical bundles essentially form a cocoon-like structure with an inner cavity, within which the palmitic acid ligand sits much like a silkworm. The cavity has a length of 27 Å and an approximate radius of 4 Å. One end of it near the carboxylate head group of palmitic acid leads to two surface openings, and the two structural water molecules (namely Wat^{36} and Wat^{268}) interact with each oxygen atom of the palmitic acid located at a different opening (Fig. 4*A*).

The palmitic acid molecule occupies most of the space within the binding cavity. None of the residues on the inner surface of the cavity are charged; most are hydrophobic, with a few exceptions being polar residues (Fig. 4*C*). Residues involved in the hydrophobic interaction network with palmitic acid are $Ile^{339A/B}$, $Ile^{335A/B}$, $Val^{316A/B}$, $Leu^{312A/B}$, $Ala^{309A/B}$, $Gln^{305A/B}$, $Leu^{302A/B}$, $Asn^{301A/B}$, $Val^{298A/B}$, $Leu^{282A/B}$, $Ile^{279A/B}$, $Ala^{278A/B}$, $Ile^{275A/B}$, $Thr^{243A/B}$, $Leu^{239B/A}$, $Leu^{233B/A}$, $Leu^{232B/A}$, $Phe^{217B/A}$, and $Ile^{210B/A}$. Aside from hydrophobic interactions, the palmitic acid within the binding cavity also forms hydrogen bonds with two bound water molecules. The first oxygen atom of the carboxyl group of bound palmitic acid forms a hydrogen bond with an ordered water molecule (Wat^{36}), which in turn forms hydrogen bonds with the hydroxyl group of the $Ser^{313A/B}$ side chain and the carbonyl group of $Ser^{332A/B}$ in LBD2. The second oxygen atom of palmitic acid forms a hydrogen bond with another water molecule (Wat^{268}) within the cavity (Fig. 4*C*).

Fatty Acid Binding Studies—The binding of long saturated fatty acids is difficult to assay accurately by titration calorimetry because of their insoluble nature. Palmitoleic acid (PA), oleic acid, and arachidonic acid were thus selected as test ligands for ITC experiments. Representative titrations of full-length Mp1p (residues 35–429) with palmitoleic acid are shown in Fig. 5. The binding isotherm was derived from integration of the peaks and fitted to a model assuming a single binding site or two independent binding sites for Mp1p. Dissociation constants and calculated entropies obtained for full-length Mp1p with three different ligands and for the LBD2 (WT and mutants) with PA are shown in Table 2. The binding stoichiometry in all cases was very close to either 1:2 (for full-length Mp1p) or 1:1 (for LBD2). The S313A and S332A mutants of LBD2 were made to disrupt the hydrogen bonding network between the carboxylate group of PA and the protein. A cloning artifact, K197Q, was found to be present in

FIGURE 3. **AUC results for WT Mp1p and WT LBD2, delipidated or with PA at different concentrations.** The AUC results are represented as a c(M) distribution model. *A*, the *blue curve* refers to WT Mp1p. *B*, the *green curve* stands for Mp1p after delipidation process. *C* and *D*, the *orange* (*C*) and *pink curves* (*D*) refer to the samples of delipidated Mp1p added with PA at molar ratio 1:2 and WT Mp1p with PA at molar ratio 1:8, respectively. *E*, the *red curve* refers to WT LBD2. *F*, the *purple curve* represents LBD2 after delipidation. *G* and *H*, the *brown* (*G*) and *gray curves* (*H*) refers to the samples of delipidated LBD2 added with PA at molar ratio 1:1 and WT LBD2 with PA at molar ratio 1:1.5, respectively.

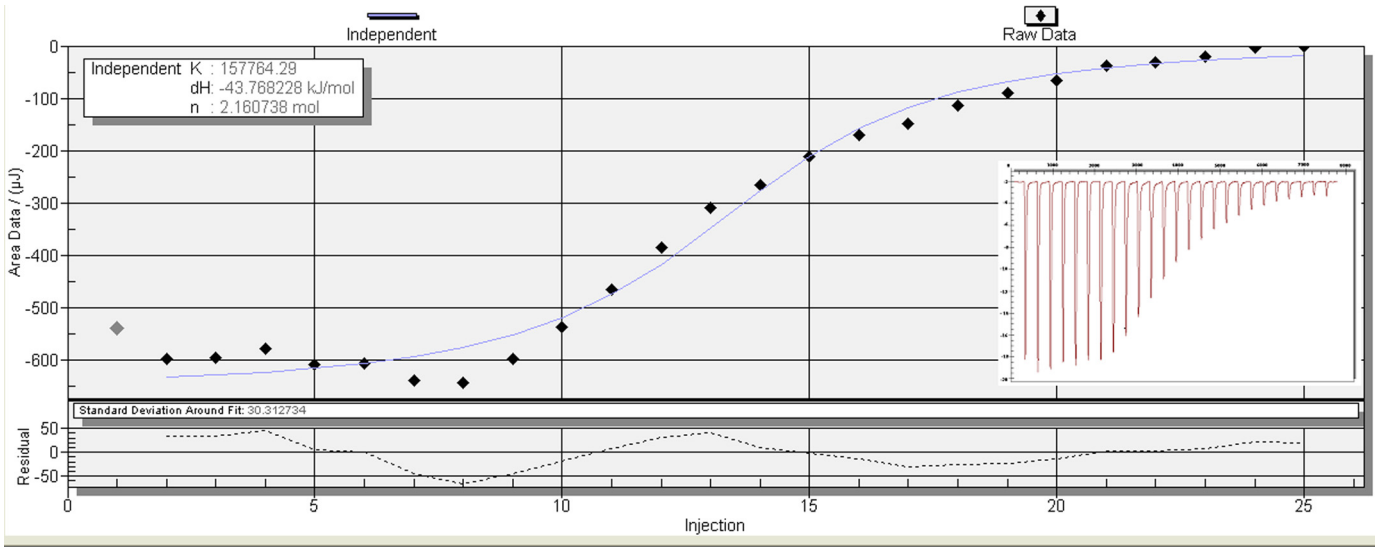

FIGURE 5. **Titration of Mp1p with PA.** Binding isotherms were derived from the raw data shown in the *insets*, with 100 μM Mp1p at 25 °C.

TABLE 2

Binding parameters of full-length pET28a-Mp1p with fatty acids and pET28a-LBD2 (WT or mutant) with palmitoleic acid

All of the binding parameters were derived from ITC assays at 25 °C as described under "Experimental Procedures." K_d is the dissociation constant, and n is the number of binding sites.

Protein	Fatty acid	K_d	ΔH	n
		μM	kJ/mol	
Mp1p	Palmitoleic acid	6.34	−43.77	2.16
Mp1p	Oleic acid	4.15	−39.38	2.21
Mp1p	Arachidonic acid	2.36	−43.99	2.31
LBD2	Palmitoleic acid	2.34	−51.58	1.00
LBD2 S313A	Palmitoleic acid	1.24	−58.48	0.69
LBD2 S313A/S332A	Palmitoleic acid	18.82	−44.50	0.76

the construct by sequencing. However, the mutation is far from the ligand binding site and does not interfere with the dimerization or other biochemical behavior of LBD2 that might affect our assays. As a result, the S313A/S332A double point mutation lowers the ligand binding affinity to 12% of the wild type LBD2. Surprisingly, the S313A mutant did not show a decrease in ligand binding affinity but increased the affinity by ~2-fold over that of the native protein. On the other hand, S332A degraded too quickly and thus could not be tested by ITC.

DISCUSSION

Overall Structure of LBD2 and Mp1p—The results of AUC experiments show that Mp1p and LBD2 are both mostly monomeric in the presence (Fig. 3, *C* and *G*) or absence (Fig. 3, *B* and *F*) of the ligand, although the addition of excess ligand increases the proportion of the dimer form (Fig. 3, *D* and *H*). According to the high occupancy of ligand based on our structure and original density map (Fig. 4*B*), WT LBD2 monomers (Fig. 3*E*) should be mostly in the ligand-bound form, as well as WT Mp1p (Fig. 3*A*). As suggested in previous reports (21), the addition of the ligand shifted the monomer-dimer equilibrium toward the dimer form, showing that the ligand binds with higher affinity to the dimer than to the monomer. It would appear that both Mp1p and LBD2 molecules remain as monomers during the ligand binding process at normal ligand concentration and only dimerize if there is excessive ligand in the protein solutions, which does not seem to be the case *in vivo*. Thus dimerization may not be biologically relevant for Mp1p.

Because the fatty acid concentration in the natural host of *P. marneffei* should be quite low, because of the nutrient deprivation of the macrophages, it is conceivable that Mp1p proteins bound with ligands exist as monomers *in vivo*, the same as LBD2 expressed in *E. coli* cells (Fig. 3*E*). Therefore a monomeric, ligand-bound LBD2 conformation must exist. However, in our crystal structure, LBD2 molecules dimerize and then form an intertwined complex, with the two helical bundles forming the ligand binding cavity from two different LBD2 molecules. This dimerization occurs most likely as a result of interaction with the high concentration of precipitant in the crystallization droplet. It is reasonable to assume that the monomeric LBD2 molecule forms its ligand binding cavity in a similar way as the dimer, namely between the two-helix bundle and the four-helix bundle. Considering the high flexibility of the loops between the two helical bundles, there is a great chance that ligand-bound LBD2 molecules exist in two different conformations. One is the extended form (Fig. 2*A*), as in our dimer structure caused by crystal packing, and the other is the closed monomeric form (Fig. 2*C*), represented by one of the two rugby ball-like shapes in the dimer structure (Fig. 2*B*). The main difference between the two conformations is the orientation of the two-helix bundle relative to the four-helix bundle in the same LBD2 molecule. Because LBD2 is mostly monomeric, the closed form may be the natural conformation of the ligand-bound LBD2 *in vitro* as well as *in vivo*. It can also explain why Mp1p is still mostly monomeric after adding enough ligand to its delipidated sample (Fig. 3*C*). A schematic for the structure of the ligand-bound LBD1 and LBD2 domains of Mp1p is shown in Fig. 2*E* based on the assumption of the closed conformation.

As a cell wall mannoprotein, Mp1p has two putative *N*-glycosylation sites, namely Asn^{209} and Asn^{429}, and a serine- and threonine-rich region for *O*-glycosylation (2). As shown by our crystal structure, Asn^{209} is on the surface of both the monomer and dimer of LBD2; thus its glycosylation will probably not hinder the process of ligand binding, whereas *N*-glycosylation

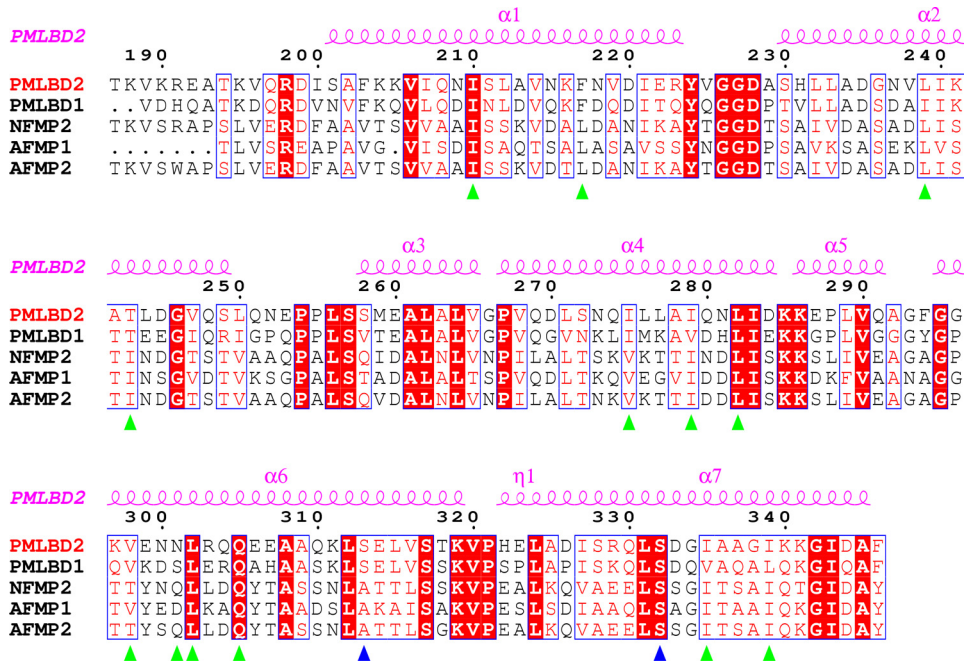

FIGURE 6. **Sequence alignment of Mp1p (*P. marneffei*) with homologous proteins.** From *top* to *bottom*, the sequences are: LBD2 of Mp1p from *P. marneffei*; LBD1 of Mp1p from *P. marneffei*; NFMP2 from *N. fischeri*; AFMP1 from *A. fumigatus*; AFMP2 from *A. fumigatus*. The last three aligned sequences are the putative LBD domains from the three different proteins. The secondary structure of Mp1p (*P. marneffei*) is indicated at the top of the alignment. Strictly conserved residues among the aligned sequences are indicated in *red*, and the most conserved residues are *shaded* in *red*. Residues involved in hydrogen bond formation or hydrophobic interaction with palmitic acid are labeled with *blue* and *green triangles*, respectively. The LBD2 residues are *numbered* above the sequence.

of Asn^{429} is at the end of the C terminus near other *O*-glycosylations in domain 3, and neither seems to be in the way of the fatty acid binding process. Taken together, it is conceivable that the fatty acid binding phenomenon observed in our domain structure is also true for Mp1p *in vivo*.

Ligand Binding—Because of the insoluble nature of long saturated fatty acids, their binding affinity to Mp1p cannot be determined accurately by ITC. Palmitoleic acid (C16:1), oleic acid (C18:1), and arachidonic acid (C20:4) were thus used as test ligands in the ITC experiments. The results show that Mp1p exhibits a strong capability for ligand binding, no matter with mono- or polyunsaturated fatty acid. However, it would appear that the binding affinity is higher for longer carbon chains, although the change is not that obvious. This may well be explained by the nature of the ligand binding cavity. As mentioned above, most of the protein residues involved in cavity formation are hydrophobic residues, thus ensuring that hydrophobic interactions are an important factor in influencing the binding affinity. Fatty acids with longer carbon chains will therefore tend to bind more tightly with Mp1p. That could also explain the high enthalpy observed in the ITC experiments. Nonetheless, hydrogen bonds are also a key factor in fatty acid binding affinity and are even more intense than hydrophobic interactions/residue. Two site-directed mutants, S313A and S332A, resulted in a 90% loss of binding of the WT protein. Interestingly, the S313A single mutation actually resulted in an obvious increase in binding affinity. It is reasonable to explain that S332A is sufficient for stabilizing the carboxylate head group, and S313A increases the hydrophobic interaction interphase, which results in an decrease in K_d. Sequence alignment with the corresponding regions in various MP1 homologs in *Aspergillus fumigatus and Neosartorya fischeri* shows that most of the residues involved in hydrophobic interactions with palmitic acid are highly conserved, indicating similar roles as fatty acid-binding proteins (Fig. 6). It is interesting to observe that Ser^{332}, mutation of which severely affected binding affinity, is strictly conserved among all five proteins, whereas Ser^{313} is not.

Biological Functions of Mp1p—As a highly abundant protein in the serum of patients with penicilliosis, it is conceivable that the biological importance of the cell wall protein Mp1p is to provide the pathogen with rich carbon resources for its metabolism and virulence. As mentioned above, *P. marneffei* has developed its own mechanism to deal with the nutrient-deficient environment of its natural host macrophage, through the activation of the glyoxylate cycle. However, that is far from sufficient because the simple carbon source can also be quite limited in macrophages after infection. Therefore, a mechanism for the snatching, transportation and enrichment of fatty acid to the pathogen surface, will also have great significance for the survival of *P. marneffei.* Because the fatty acid concentration in the host should be low, it is reasonable to assume that Mp1p molecules will exist mostly as monomers *in vivo*. However, the influence of glycosylation should not be neglected because it may play a vital role in the monomer-dimer equilibration. Mp1p is comprehensively located at the cell wall of the yeast, hyphae, and conidia of *P. marneffei*, as well as in patient serum at high concentrations. It binds fatty acid with high affinity and low specificity regardless of their length. All of the above features imply the role of Mp1p as a fatty acid transporter from the host to the pathogen itself (Fig. 7). This can be mirrored by the function of Ag-lbp55 from *Ascaridia galli* (22). Mp1p and Ag-lbp55 are similar in several aspects. First, they are both helical antigenic proteins. Second, they both show high affinity for amphipathic molecules such as fatty acids. Third, they are both highly abundant and secreted into host tissues. The phenomenon of lipid snatching from host cells can also be observed in the apicomplexan parasites (23).

The fatty acid binding feature may also explain the phenomenon observed in previous research work, whereby Mp1p was present throughout the thickness of the conidial cell walls but only localized on the outer layer of the hyphal cell walls (2). Conidiation occurs when conditions are no longer suitable for hyphal growth (24). Nutrient starvation, including carbon limitation, is the most widely accepted environmental stimulus leading to conidiation. The fatty acid binding properties of Mp1p and its wide existence throughout the conidia cell wall

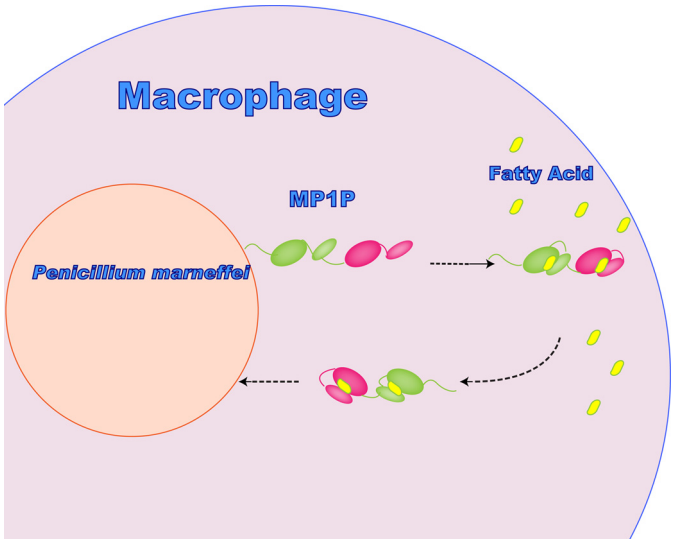

FIGURE 7. **Possible mode of action of *P. marneffei* Mp1p in fatty acid host-pathogen trafficking.** LBD1 and LBD2 are colored *pink* and *green*, respectively. The four-helix bundles are represented by *larger ovals*, whereas the two-helix bundles are represented by *smaller ovals*. The fatty acids are indicated as *small yellow ovals*.

led to the assumption that it acts as a carbon resource for conidia, which would confer great tolerance against nutrient starvation. It also explains why Mp1p is distributed evenly throughout the thickness of the cell wall of the yeast form. Because the yeast form is considered to be the infectious form in humans, it has to encounter the nutrient-deficient environment created by the host macrophages, similar to the situation for conidia. Therefore, they exhibit similar patterns of Mp1p distribution in the cell walls compared with the hyphal forms, in which Mp1p mainly exists in the outer layer and acts as a fatty acid transporter.

Acknowledgments—We thank Zheng Fan (Institute of Microbiology, Chinese Academy of Sciences) for support in isothermal titration calorimetry. We thank Chengdui Yang (Analysis Center, Tsinghua University) for support with GC/MS experiments. We also thank Xiaoxia Yu (Institute of Biophysics, Chinese Academy of Sciences) for support in the analytical ultracentrifugation experiments. We are grateful to Zhiyong Lou for help with data collection and processing and Sheng Fu for technical assistance.

REFERENCES

1. Yuen, K. Y., Pascal, G., Wong, S. S., Glaser, P., Woo, P. C., Kunst, F., Cai, J. J., Cheung, E. Y., Médigue, C., and Danchin, A. (2003) *Arch. Microbiol.* **179,** 339–353
2. Cao, L., Chan, C. M., Lee, C., Wong, S. S., and Yuen, K. Y. (1998) *Infect. Immun.* **66,** 966–973
3. Cao, L., Chan, K. M., Chen, D., Vanittanakom, N., Lee, C., Chan, C. M., Sirisanthana, T., Tsang, D. N., and Yuen, K. Y. (1999) *J. Clin. Microbiol.* **37,** 981–986
4. Cao, L., Chen, D. L., Lee, C., Chan, C. M., Chan, K. M., Vanittanakom, N., Tsang, D. N., and Yuen, K. Y. (1998) *J. Clin. Microbiol.* **36,** 3028–3031
5. Wong, S. S., Wong, K. H., Hui, W. T., Lee, S. S., Lo, J. Y., Cao, L., and Yuen, K. Y. (2001) *J. Clin. Microbiol.* **39,** 4535–4540
6. Woo, P. C., Lau, C. C., Chong, K. T., Tse, H., Tsang, D. N., Lee, R. A., Tse, C. W., Que, T. L., Chung, L. M., Ngan, A. H., Hui, W. T., Wong, S. S., Lau, S. K., and Yuen, K. Y. (2007) *J. Clin. Microbiol.* **45,** 3647–3654
7. Appelberg, R. (2006) *J. Leukocyte Biol.* **79,** 1117–1128
8. Lorenz, M. C., and Fink, G. R. (2002) *Eukaryot. Cell* **1,** 657–662
9. Cánovas, D., and Andrianopoulos, A. (2006) *Mol. Microbiol.* **62,** 1725–1738
10. Darios, F., Connell, E., and Davletov, B. (2007) *J. Physiol.* **585,** 699–704
11. Wenk, M. R. (2006) *FEBS Lett.* **580,** 5541–5551
12. Otwinoswki, Z., and W. Minor. (1997) *Processing of X-ray Diffraction Data Collected in Oscillation Mode* (Carter, C. W., Jr., and Sweet, R. M., eds) pp. 307–326, Academic Press, New York
13. Rice, L. M., Earnest, T. N., and Brunger, A. T. (2000) *Acta Crystallogr. D Biol. Crystallogr.* **56,** 1413–1420
14. Morris, R. J., Perrakis, A., and Lamzin, V. S. (2003) *Methods Enzymol.* **374,** 229–244
15. Emsley, P., and Cowtan, K. (2004) *Acta Crystallogr. D Biol. Crystallogr.* **60,** 2126–2132
16. Murshudov, G. N., Vagin, A. A., and Dodson, E. J. (1997) *Acta Crystallogr. D Biol. Crystallogr.* **53,** 240–255
17. Balendiran, G. K., Schnutgen, F., Scapin, G., Borchers, T., Xhong, N., Lim, K., Godbout, R., Spener, F., and Sacchettini, J. C. (2000) *J. Biol. Chem.* **275,** 27045–27054
18. Schuck, P. (2000) *Biophys. J.* **78,** 1606–1619
19. Berman, H. M., Westbrook, J., Feng, Z., Gilliland, G., Bhat, T. N., Weissig, H., Shindyalov, I. N., and Bourne, P. E. (2000) *Nucleic Acids Res.* **28,** 235–242
20. Holm, L., Kaariainen, S., Wilton, C., and Plewczynski, D. (2006) *Current Protocol Bioinformatics*, Chapter 5, Unit 5.5
21. Schymkowitz, J. W., Rousseau, F., Wilkinson, H. R., Friedler, A., and Itzhaki, L. S. (2001) *Nat. Struct. Biol.* **8,** 888–892
22. Jordanova, R., Radoslavov, G., Fischer, P., Torda, A., Lottspeich, F., Boteva, R., Walter, R. D., Bankov, I., and Liebau, E. (2005) *J. Biol. Chem.* **280,** 41429–41438
23. Mazumdar, J., and Striepen, B. (2007) *Eukaryot. Cell* **6,** 1727–1735
24. Roncal, T., and Ugalde, U. (2003) *Res. Microbiol.* **154,** 539–546